Molecular simulation of the carbon nanotube growth mode during catalytic synthesis

Soumik Banerjee, Sayangdev Naha, and Ishwar K. Puri

Citation: Applied Physics Letters **92**, 233121 (2008); doi: 10.1063/1.2945798
View online: http://dx.doi.org/10.1063/1.2945798
View Table of Contents: http://scitation.aip.org/content/aip/journal/apl/92/23?ver=pdfcov
Published by the AIP Publishing

Molecular simulation of the carbon nanotube growth mode during catalytic synthesis

Soumik Banerjee, Sayangdev Naha, and Ishwar K. Puri[a)]
Department of Engineering Science and Mechanics, Virginia Polytechnic Institute and State University, Blacksburg, Virginia 24061-0219, USA

(Received 25 April 2008; accepted 22 May 2008; published online 13 June 2008)

Catalyzed growth of carbon nanostructures occurs mainly through two modes, i.e., base growth when the metal nanoparticle remains at the bottom of the nanotube, or when it is lifted by the growing carbon nanostructure due to tip growth. A correct prediction of the dominant growth mode depends on the energy gain due to the addition of C atoms from the carbon-metal catalyst solution to the graphene sheets forming the carbon nanostructures. We determine this energy gain through atomistic scale molecular dynamics simulations. Our results suggest tip growth for Ni and base growth for Fe catalysts. © *2008 American Institute of Physics*. [DOI: 10.1063/1.2945798]

A carbon deposit can be created at elevated temperatures on catalytically active transition metal nanoparticles that are placed in a reducing environment with high gas-phase carbon activity.[1,2] The deposited carbon diffuses into the catalyst nanoparticle, nucleates within it, and emerges in the form of carbon nanotubes (CNTs) or nanofibers (CNFs). The subsequent catalyzed growth of CNTs and CNFs occurs mainly through two modes. The base growth mode arises when the metal nanoparticle catalyzing the growing carbon nanostructure remains at the bottom of the nanotube. For this type of growth, the adhesive forces between the substrate and the catalyst nanoparticle are typically too large for the particle to be lifted as the CNT/CNF grows. Alternately, the catalyst nanoparticle is lifted by the growing carbon nanostructure during tip growth, and remains at the tip of the CNT/CNF after its growth ceases.

The nature of the growth mode, whether tip or base, is important for various applications. For instance, the nucleation of metal particles on the end caps of CNTs can assist in the alignment of these nanostructures in the presence of external electric or magnetic fields, thus imparting directional properties to materials in which these are embedded.[3,4] Such functionalized tips can also be used to attract other molecules for various applications, e.g., for functionalization with protonated amines ($-NH_3^+Cl^-$) that add positive charges to CNTs, which allows binding to negatively charged RNA molecules.[5] Continuum scale CNT growth models that typically assume a certain growth mode[6] can also benefit from these predictions.

Illustrations of the two growth modes are presented in the supplementary material.[7] The likely growth (tip or base) mode depends on the energy gain $\Delta E_{np\rightarrow \mathrm{CNT}}$ due to the addition of C atoms from the carbon-metal catalyst solution to the graphene sheets forming the CNTs and CNFs. For tip growth to occur, the catalyst particle is lifted from a substrate only if the energy gain is sufficient to overcome the surface binding or interface energy between the nanoparticle and the substrate, i.e., $\Delta E_{np\rightarrow \mathrm{CNT}} \geqslant \gamma R_p^2$, where γ and R_p denote the surface energy per unit area and the radius of the metal catalyst particle, respectively. Smaller energy gains lead to base growth. The prediction of the dominant growth mode for a specific condition requires that $\Delta E_{np\rightarrow \mathrm{CNT}}$ be determined using molecular dynamics (MD) simulations. We justify either growth mode on the predicted energy gain, an analysis that we find to be more robust than one based on characteristic time scale considerations.

The experimentally observed base growth mode by Wu *et al.* was facilitated by an Fe catalyst immersed in C_2H_4 with a $\approx$162.86 torr partial pressure and 1048 K temperature.[8] The other gaseous species were H_2 (carrier gas) and Ar (inert). The experimental results of Ducati *et al.* revealed a predominance of vertically aligned CNTs grown through a tip-growth mode with Ni as catalyst and C_2H_2 as the carbon source gas at a temperature of 823 K and 1.5 torr partial pressure.[9] Our simulations correspond to conditions for these two representative cases.

Our simulations are based on the massively parallel LAMMPS code.[10] The interaction between the carbon atoms in the metal and the nanotube are modeled using the adaptive intermolecular reactive empirical bond order (AIREBO) potential

$$E = \frac{1}{2}\sum_i \sum_{j\neq i} \left[E_{ij}^{\mathrm{REBO}} + E_{ij}^{LJ} + \sum_{k\neq i,j} \sum_{l\neq i,j,k} E_{kijl}^{\mathrm{torsion}} \right]. \quad (1)$$

The E^{REBO} term has the same functional form as the hydrocarbon REBO potential.[11] The E^{LJ} term adds longer-range interactions ($2\ \text{Å} < r < r_{\mathrm{cutoff}}$) using a form similar to the standard Lennard–Jones (LJ) potential. The E^{torsion} term is an explicit four-body potential that describes various dihedral angle preferences in hydrocarbon configurations. The Ni–Ni and Fe–Fe interactions are modeled using the embedded atom model (EAM) potential,

$$E_i = F_\alpha \left[\sum_{j\neq i} \rho_\alpha(r_{ij}) \right] + \frac{1}{2}\sum_{j\neq i} \phi_{\alpha\beta}(r_{ij}), \quad (2)$$

where F denotes the embedding energy, which is a function of the atomic electron density ρ, φ is a pair potential interaction, and α and β are the element types of atoms i and j. The multibody nature of the EAM potential is a result of the embedding energy term. Both summations in the formula are over all neighbors j of atom i within the cutoff distance

[a)]Author to whom correspondence should be addressed. Tel.: +1-540-231-3243. FAX: +1-540-231-4574. Electronic mail: ikpuri@vt.edu.

TABLE I. LJ interaction parameters for Fe, Ni, C, and Ar.

Interaction parameters	ε (eV)	σ (Å)
Ar–Ar	0.0103	3.4
Ar–Ni	0.1426	3.57
Ar–Fe	0.0516	3.7
C–Ar	0.004 97	3.4
C–Ni	0.0688	3.57
C–Fe	0.024 95	3.7

r_{cutoff}. The interactions between Ar–Ar, Ar–Ni/Fe, Ar–C, and Ni–C are modeled using a LJ potential,

$$E_{ij} = 4\varepsilon_{ij}[(\sigma_{ij}/r_{ij})^{12} - (\sigma_{ij}/r_{ij})^{6}]. \quad (3)$$

In Eq. (3), r_{ij} denotes the scalar distance between sites i and j, and σ_{ij} and ε_{ij} are the LJ interaction parameters obtained from the literature[12,13] and are listed in Table I for various cases.

Our simulation configuration is schematically described in Fig. 1. The $13.75 \times 2.75 \times 54.8$ nm^3 cuboid domain consists of a (10, 10) single-walled armchair CNT of 1.375 nm diameter, 2.74 nm in length, and 2.49 Å pore size. The CNT, placed on top of a Ni or Fe nanoparticle with dissolved C atoms, is surrounded with an Ar ambient. Thus, the simulations model experimental conditions following carbon diffusion into the metal catalyst and its subsequent nucleation. The C atom concentration in the metal is 6.67% for both cases. The system temperature is varied between 700 and 1100 K, and the pressure is maintained at 760 torr (1 atm). Periodic conditions apply to the boundaries in order to eliminate wall effects so that the system is effectively infinite in all directions.

A typical simulation for a Fe nanoparticle consists of 6825 Fe atoms, 2748 C atoms, 44 Ar atoms, and the CNT. A similar simulation for Ni consists of 8253 Ni atoms, 2275 C atoms, 44 Ar atoms, and the CNT. Initially, all molecules that are not part of the CNT form a face-centered-cubic (fcc) lattice that equilibrates through the simulations. A thermostat maintains constant temperature so that the molecules have an initial velocity distribution corresponding to the system temperature. A cutoff distance of 3 Å for the AIREBO and 6 Å for the LJ potential is used. Once the configuration equilibrates, we calculate the total energy of the carbon atoms that have attached to the CNT, since the difference between the initial and final energies of these atoms equal $\Delta E_{np\rightarrow\text{CNT}}$.

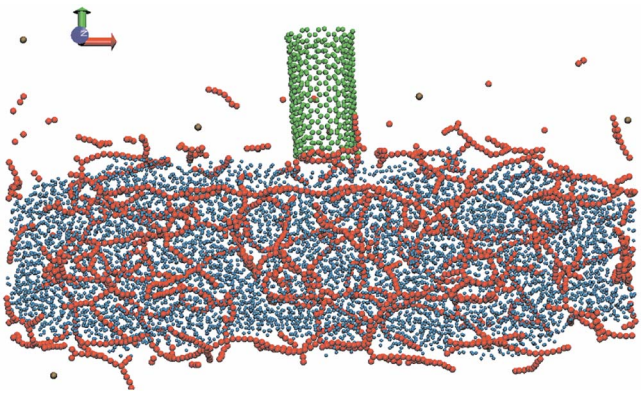

FIG. 1. (Color online) A two-dimensional orthographic view of the MD simulation domain with the CNT (green), which is surrounded by ambient Ar (gray), growing on top of the metal catalyst particle (blue) that has dissolved carbon (red).

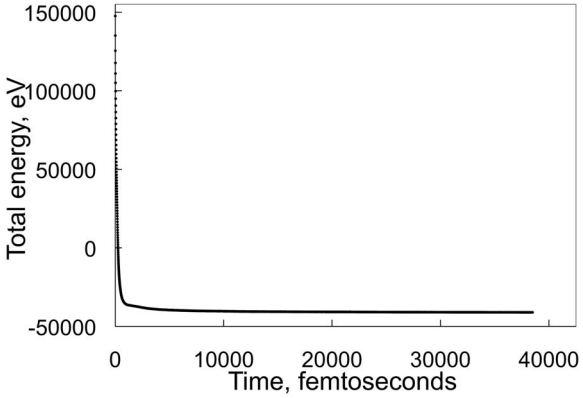

FIG. 2. The variation of the total system energy with time.

The time evolution of the total system energy for the Fe nanoparticles at 800 K is presented in Fig. 2. The system energy reaches a minimum value and remains constant after 75 femtoseconds (fs). We sample data between 8 500 fs and 18 500 fs, which is well beyond this equilibration time, to obtain the equilibrium energy values for the various cases. The initial energy of the carbon atoms dissolved in the catalyst particle is likewise sampled between 100 fs and 2 500 fs, and the corresponding average values are reported.

Figure 3 presents the temperature dependence of $\Delta E_{np\rightarrow\text{CNT}}$ for both Fe and Ni catalysts. In the case of Fe, the magnitude of the energy change decreases with an increase in temperature between 700 and 900 K, but is thereafter constant at higher temperatures. The specific surface energy for Fe $\gamma = 0.17$ eV/Å^2 (Ref. 14) so that the surface interaction energy for a typical 10 nm Fe catalyst particle $\gamma R_p^2 \approx 1700$ eV. For temperatures between 700 and 1100 K, $\Delta E_{np\rightarrow\text{CNT}} < 600$ eV, since $\Delta E_{np\rightarrow\text{CNT}} < \gamma R_p^2$, this indicates a base growth mode. There is a weak temperature dependence of the energy change in the case of Ni and $\Delta E_{np\rightarrow\text{CNT}} > 125$ eV over the entire temperature range. For Ni, $\gamma = 0.125$ eV/Å^2, i.e., for a typical 3 nm Ni catalyst particle, $\gamma R_p^2 \approx 113$ eV, which is smaller in value than $\Delta E_{np\rightarrow\text{CNT}}$. Hence, the energy change due to bond formation is large enough to induce tip growth.

It has been suggested that the growth mode depends upon two characteristic times, respectively, the diffusion and surface saturation times $\tau_d \approx R_p^2/D_b$ and $\tau_s \approx C^{*2}D_b/Q^2$.[15]

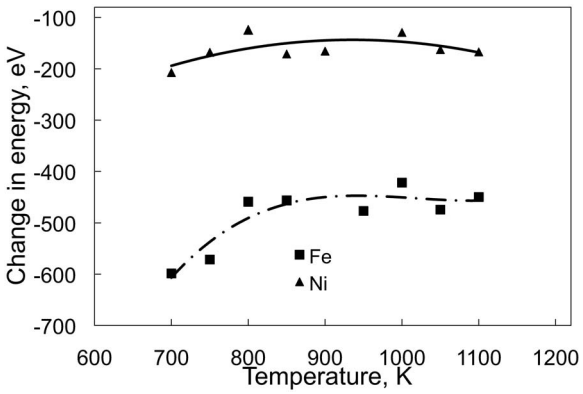

FIG. 3. The variation of the energy change with respect to temperature for Ni and Fe.

Here, D_b represents carbon bulk diffusivity in the metal catalyst, C^* the carbon saturation concentration in the metal catalyst particle (in terms of number of particles per unit volume), $Q=P_c/(2\pi mk_BT)^{1/2}$ the carbon flux, P_c, T, and m the partial pressure, temperature, and molecular mass of the carbon-containing gas, respectively, and k_B the Boltzmann constant.

The two abovementioned experimental studies[8,9] offer model examples of how these time scales can be used to predict the correct growth mode for one case but not for the other. The overall adsorption rate of C atoms $Q=N_{c,i}\nu$, where $N_{c,i}$ represents the impingement rate and ν the sticking coefficient of a particular hydrocarbon species.[16,17] The sticking coefficient is defined as the probability of occurrence of a particular reaction through a favorable intermolecular collision.[16,18] The impingement rate $Q=\nu.jN_{\mathrm{Av}}P/\sqrt{2\pi MRT}=\nu.3.513jP/\sqrt{MT}\times 10^{22}$, where j denotes the number of carbon atoms contained in each molecule of the predominant gas-phase hydrocarbon species (e.g., $j=2$ for C_2H_4, which is the only carbon-containing gas in this case), M its molecular weight, P its near-surface partial pressure, and T its temperature (assumed to be the same as of the substrate), N_{Av} the Avogadro number, and R the universal gas constant. Here, $\nu=0.2$,[18] $T=1048$ K, $M=28$, and $P=162.86$ torr, $Q\approx 1.336\times 10^{22}$ for the conditions reported by Wu *et al.*[8]

The bulk diffusivity of carbon in iron $D_b\cong D_0\exp[-\delta E_b/(k_BT)]$, where $D_0\approx 0.1-0.5$ cm^2/s and $\delta E_b\approx 137-153$ kJ/mol for $T=1000-1500$ K.[19] Thus, D_b lies in the range $(0.6118-3.06)\times 10^{-8}$ cm^2/s, assuming that $C^*\approx 2.196\times 10^{22}$ cm^{-3}, $a_0\approx 10^{-8}$ cm (or 1 Å), $\tau_d\approx 1.225\times 10^{-6}$ s and $\tau_S\approx 4.6\times 10^{-8}$ s. Since the time scale for bulk diffusion is two orders of magnitude greater than the characteristic surface saturation time, i.e., $\tau_d\gg\tau_S$, surface saturation occurs before the C atoms diffuse into the nanoparticle and such an analysis predicts the base growth mode. This is indeed observed experimentally.[8]

A similar use of the time scales offers an incorrect growth mode prediction in the case of the Ni-catalyzed growth conditions.[9] Assuming a typical catalyst particle diameter of 3 nm by observing the CNT inner diameters, and values of $D_0=0.1$ cm^2/s and $E_d=33$ kcal/mol (Ref. 20) in the D_b relation for carbon diffusion in Ni, $\tau_d\approx 1.322\times 10^{-4}$ s and $\tau_S\approx 5.77\times 10^{-6}$ s. Since $\tau_d\gg\tau_S$, the carbon concentration at the surface is always predicted to increase, similar to the previous case for Fe. Consequently, the time scale analysis predicts a base growth mode for this case although there is contrary experimental evidence of tip growth.[9] We use this discussion to emphasize that the value of $\Delta E_{np\rightarrow \mathrm{CNT}}$ should be determined based on classical MD simulations.

In summary, we have investigated the growth modes of CNTs using atomistic MD simulations and validated our results against experimental evidence. The MD results suggest different growth modes for Ni and Fe catalysts. While the magnitude of energy gain for a wide range of temperatures typically encountered in catalyzed CNT growth is smaller than the surface interaction energy for Fe, the converse is true for Ni. Our results suggest that Ni catalyst nanoparticles are conducive for tip growth while Fe nanoparticles promote base growth. Use of Ni produces a local minimum energy at approximately 900 K while for Fe-catalyzed growth, the energy gain decreases to a constant minimum value at temperatures exceeding 900 K. A phenomenological time scale is insufficient to definitively characterize the nature of the growth mode. Thus, it is imperative to quantify the energy gain due to the addition of carbon atoms to a CNT based on more fundamental considerations.

We thank the Virginia Tech Advanced Research Computing Facility for use of the terascale System X.

[1] A. Sacco, P. Thacker, T. N. Chang, and A. T. S. Chiang, J. Catal. **85**, 224 (1984).
[2] A. J. H. M. Kock, P. K. de Bokx, E. Boellaard, W. Klop, and J. W. Geus, J. Catal. **96**, 468 (1985).
[3] J. H. Park, P. S. Alegaonkar, S. Y. Jeon, and J. B. Yoo, Compos. Sci. Technol. **68**, 753 (2008).
[4] E. Camponeschi, R. Vance, M. Al-Haik, H. Garmestani, and R. Tannenbaum, Carbon **45**, 2037 (2007).
[5] R. Krajcik, A. Jung, A. Hirsch, W. Neuhuber, and O. Zolk, Biochem. Biophys. Res. Commun. **369**, 595 (2008).
[6] Y. Zhang and K. J. Smith, J. Catal. **231**, 354 (2005).
[7] See EPAPS Document No. E-APPLAB-92-092824 for illustrations of the two growth modes of carbon nanotubes. For more information on EPAPS see, http://www.aip.org/pubservs/epaps.html
[8] J. Wu, Q. W. Huang, Y. F. Ma, Y. Huang, Z. F. Liu, X. Y. Yang, Y. S. Chen, and D. P. Chen, Colloids Surf., A **313**, 13 (2008).
[9] C. Ducati, I. Alexandrou, M. Chhowalla, J. Robertson, and G. A. J. Amaratunga, J. Appl. Phys. **95**, 6387 (2004).
[10] S. Plimpton, J. Comput. Phys. **117**, 1 (1995).
[11] D. W. Brenner, O. A. Shenderova, J. A. Harrison, S. J. Stuart, B. Ni, and S. B. Sinnott, J. Phys.: Condens. Matter **14**, 783 (2002).
[12] P. Nigra, D. L. Freeman, D. Sabo, and J. D. Doll, J. Chem. Phys. **121**, 475 (2004).
[13] C. H. Turner, J. K. Brennan, J. Pikunic, and K. E. Gubbins, Appl. Surf. Sci. **196**, 366 (2002).
[14] L. Vitos, A. V. Ruban, H. L. Skriver, and J. Kollár, Surf. Sci. **411**, 186 (1998).
[15] O. A. Louchev, T. Laude, Y. Sato, and H. Kanda, J. Chem. Phys. **118**, 7622 (2003).
[16] S. Naha and I. K. Puri, J. Phys. D: Appl. Phys. **91**, 065304 (2008).
[17] S. Naha, S. Sen, A. K. De, and I. K. Puri, Proc. Combust. Inst. **31**, 1821 (2007).
[18] H. Liu and D. S. Dandy, J. Electrochem. Soc. **143**, 1104 (1996).
[19] O. A. Louchev, Y. Sato, and H. Kanda, Appl. Phys. Lett. **80**, 2752 (2002).
[20] L. H. F. A. List, D. F. Kee, K. J. Leonard, and A. Goyal, J. Mater. Res. **20**, 9 (2005).